Semifunctional Site-Specific Mutants Affecting the Hydrolytic Half-Reaction of Microsomal Epoxide Hydrolase†

Huey-Fen Tzeng, L. Timothy Laughlin, and Richard N. Armstrong*

Departments of Biochemistry and Chemistry and Center in Molecular Toxicology, Vanderbilt University School of Medicine, Nashville, Tennessee 37232-0146

Received November 5, 1997; Revised Manuscript Received January 5, 1998

ABSTRACT: Microsomal epoxide hydrolase (MEH) is a member of the α/β-hydrolase fold family of enzymes, each of which has a catalytic triad consisting of a nucleophile involved in the formation of a covalent intermediate and a general base and charge relay carboxylate that catalyze the hydrolysis of the intermediate. The rate-limiting step in the catalytic mechanism of MEH is hydrolysis of the ester intermediate. An efficient bacterial expression system for a C-terminal hexahistidine tagged version of the native enzyme, which facilitates the isolation of mutant enzymes in which residues involved in the hydrolytic half-reaction have been altered, is described. The H431S mutant of this enzyme is efficiently alkylated by substrate to form the ester intermediate but is unable to hydrolyze the ester to complete the catalytic cycle, a fact that confirms that H431 acts as the base in the hydrolytic half-reaction. The charge relay carboxylate, which is not apparent in paired sequence alignments with other α/β-hydrolase fold enzymes, is thought to be located between residues 340 and 405. A mutagenic survey of all eight Asp and Glu residues in this region reveals that only two (E376 and E404) influence the catalytic mechanism. Steady-state and pre-steady-state kinetic analyses of these residues suggest that both E404 and E376 may serve the charge relay function in the hydrolysis half-reaction. Finally, the tryptophan residue (W150), which resides in the oxyanion hole sequence HGWP, is demonstrated to contribute to the large change in intrinsic protein fluorescence observed when the enzyme is alkylated.

Microsomal epoxide hydrolase (MEH)[1] is a member of a the α/β-hydrolase fold family of enzymes (*1*, *2*). More specifically, the enzyme belongs to a subfamily of C−X bond hydrolases which function by formation of an alkyl-enzyme intermediate (*2*). The reaction mechanism of the enzyme with most substrates involves the rapid alkylation of D226 followed by rate-limiting hydrolysis of the ester intermediate (*3*−*5*). The hydrolytic half-reaction involves three structural elements, a general base and charge relay which serve to activate the water molecule and an oxyanion hole to stabilize the tetrahedral intermediate. Sequence alignments and the organization of the catalytic elements in the α/β-hydrolase fold family have been used to propose specific roles for particular residues in catalysis. For example, sequence alignments clearly identify the motif HGWP in which the main chain NH of W150 participates in the oxyanion hole. Local sequence alignments and the location of H431 near the C-terminus strongly suggest that this residue acts as the general base in the hydrolysis of the alkyl-enzyme intermediate as illustrated in Figure 1 (*2*, *3*, *6*). This notion is buttressed by the seminal findings of Bell and Kasper (*8*) that H431 is the only histidine residue in MEH that is essential for catalysis. In contrast, the identity of the charge relay carboxylate is not apparent from the sequence alignments and is probably obscured by the sequence excursions from the basic α/β-hydrolase fold that comprises the cap domain of the enzyme (*1*, *9*).

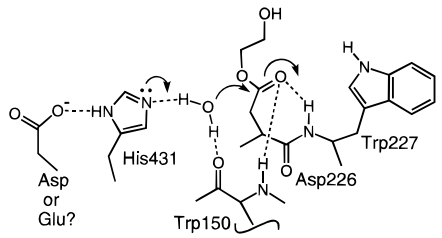

FIGURE 1: Proposed active site for microsomal epoxide hydrolase based on sequence alignments with other α/β-hydrolase fold enzymes (*2*, *3*, *6*) and the three-dimensional structure of haloalkane dehalogenase (*7*). The alkyl-enzyme intermediate is shown poised for the hydrolysis half-reaction.

Although there is considerable experimental support for the catalytic role of specific residues in the soluble epoxide hydrolases (*10*, *11*), that support is largely lacking in the case of the microsomal enzyme. A pre-steady-state kinetic analysis of the two-step mechanism of mutant enzymes provides a unique opportunity to assign specific catalytic roles to particular residues identified by sequence alignments and other considerations (*5*). For example, mutations of

† This work was supported in part by NIH Grants R01 GM49878 and P30 ES00267. L.T.L. is supported by NRSA Fellowship F32 GM18296 from the National Institute of General Medical Sciences.

* Address correspondence to this author. Phone: (615) 343-2920. FAX: (615) 343-2921. Email: armstrong@toxicology.mc.vanderbilt.edu.

[1] Abbreviations: MEH, microsomal epoxide hydrolase; chtMEH, C-terminal His·Tag microsomal epoxide hydrolase; MOPS, 3-(*N*-morpholino)propanesulfonic acid; PCR, polymerase chain reaction; LB, Luria broth; OD, optical density; HPLC, high-performance liquid chromatography; SDS−PAGE, sodium dodecyl sulfate−polyacrylamide gel electrophoresis.

S0006-2960(97)02738-4 CCC: $15.00 © 1998 American Chemical Society
Published on Web 02/07/1998

residues involved in the hydrolytic half-reaction would be anticipated to impair turnover of the enzyme but perhaps have a minimal effect on the efficiency of the alkylation reaction.

In this paper, we describe a pre-steady-state kinetic analysis of microsomal epoxide hydrolase directed at determining the specific role H431 in catalysis and the identification of the charge relay carboxylate through the construction of semifunctional site-specific mutants. The analysis is facilitated by the construction of a new bacterial expression vector encoding a C-terminal His·Tag version of the enzyme which permits the isolation of mutant enzymes difficult to purify by conventional techniques. The results indicate that H431 is not essential for the alkylation half-reaction but is absolutely required for the hydrolytic half-reaction. Analysis of several mutants of residues with carboxylate side chains in the region of sequence suspected of harboring the charge relay residue suggests that E376 and/or E404 serves this function.

EXPERIMENTAL PROCEDURES

General Materials and Methods. All reagents, buffers, solvents, enzymes, and substrates including the (2*R*)- and (2*S*)-enantiomers of glycidyl-4-nitrobenzoate, **1**, and phenanthrene 9,10-oxide, **3**, were obtained as previously described (*5*) unless otherwise noted. The general methods for vector construction, DNA sequencing, mutagenesis, protein expression, and purification and enzyme kinetic analysis are the same as those used before (*5*) unless specifically described below.

Expression Vector for C-Terminal Hexahistidine Tag Version of MEH. The cDNA sequence of MEH was amplified by the polymerase chain reaction using the synthetic oligomers 5′-AAA CTC GAG GTC GAC ACA TAT GTG GCT GGA ACT TGT CCT GGC-3′ and 5′-TTT GAA TTC CTC GAG CTG CAG CTC AGC CAG GGA CAC GAA-3′ as N-terminal and C-terminal primers, respectively. These primers were designed to create an *Nde*I site immediately 5′ to the start codon and an *Xho*I site immediately 3′ to the last codon of native MEH for subcloning into the pET20b(+) vector. The amplification was performed for 20 cycles as follows: denaturation at 92 °C for 45 s, annealing at 50 °C for 45 s, and primer extension at 72 °C for 80 s. The PCR product was then digested with *Nde*I and *Xho*I, purified, and ligated into pET20b(+) which had been digested with the same enzymes to generate pET20MEH2. The vector encoded native epoxide hydrolase plus the sequence LEHHHHHH.

Expression and Purification of Epoxide Hydrolase. E. coli BL21(DE3) cells were transformed with pET20MEH2 and plated out on LB−ampicillin (100 μg/mL) plates. A single isolated colony was picked to inoculate 100 mL of LB media containing 100 μg/mL ampicillin. A starter culture, incubated at 37 °C until the OD_{600} reached 0.2, was used to inoculate 2 L of LB−ampicillin (100 μg/mL) in a fermentor which was grown until the OD_{600} reached 0.6−1.0, at which time 12 g/L lactose was added. After 5 h, the cells were harvested by centrifugation at 6000*g* for 15 min at 4 °C and stored at −20 °C. All steps of the purification were performed at 4 °C or on ice. The cell pellet from 1 L of cell culture was resuspended in 40 mL of 5 mM imidazole, 0.5 M NaCl, 20 mM Tris-HCl (pH 7.9) (buffer A) and sonicated with four 20 s bursts at 80% power with a Branson Sonifier. The lysate was centrifuged at 20000*g* for 15 min. The pellet was resuspended in the same buffer, sonicated, and centrifuged again. The pellet was extracted twice with 6 mL of buffer A containing 0.5% Genapol C-100 followed by centrifugation at 39000*g* for 20 min. The extract was loaded on a column containing 1.5 mL of His·Bind resin (from Novagen) which had been equilibrated with buffer A. The column was washed with 15 mL of buffer A and then 9 mL of 60 mM imidazole, 0.5 M NaCl, 20 mM Tris-HCl (pH 7.9). The protein was eluted with 1 M imidazole, 0.5 M NaCl, 20 mM Tris-HCl (pH 7.9). Those fractions containing a high concentration of protein were combined, dialyzed overnight against 10 mM Tris-HCl (pH 7.6), and stored at −20 °C.

Purification of the E376Q Mutant of chtMEH. All purification steps were the same as described above for chtMEH, except the final dialysis step. To promote a more rapid dialysis, a dialysis membrane with a higher molecular weight cutoff (50 000 instead of 6000) was used. The dialysis buffer [50 mM MOPS (pH 7.0) containing 0.5 M NaCl] was changed 7 times at 60−90 min intervals. The dialyzed mutant was filtered through a 0.2 μm microfilter (Amicon) before use in steady-state and pre-steady-state kinetic experiments.

Pre-Steady-State Kinetics of chtMEH and chtE376Q with Phenanthrene 9,10-oxide. The hydrolysis of **3** by the E376Q mutant of chtMEH was followed by stopped-flow fluorescence using an Applied Photophysics SX17MV spectrometer with excitation at 270 nm. Fluorescence emission from the ester intermediate and product was observed through a 320 nm cutoff filter. The reactions were performed at 25 °C in 50 mM MOPS (pH 7.0) containing 0.5 M NaCl. Kinetic constants under single turnover conditions were obtained by fitting the progress curve using the FITSIM and KINSIM programs (*12, 13*).

RESULTS

Heterologous Expression and Purification of Epoxide Hydrolase. Mutations in the regions of MEH thought to be involved in the hydrolysis of the ester intermediate often, though not always, result in proteins that either do not express well or are difficult to purify in sufficient yield using the techniques previously described for the native enzyme. For example, of five mutants made at position 431 (H431N, H431Q, H431S, H431A, and H431G), only H431S was isolable in reasonable yield but with a purity of only 70%. For this reason, an alternative expression and purification protocol using the His·Tag methodology was developed. The resulting construct encoded the octapeptide sequence LEHHHHHH appended to the C-terminus of the enzyme which allowed purification of the protein on a nickel chelate column. The technique works well with the native enzyme and allows facile isolation of 4−5 mg of homogeneous enzyme per liter of cell culture. This is about 4-fold more efficient than the protocol for native MEH (*5*).

The catalytic characteristics of the hexahistidine-tag version of the native enzyme are very similar but not identical to those of the native protein as shown in Table 1. The turnover numbers with **3** are essentially the same, 1.1 and

Table 1: Rate Constants for the Enzyme-Catalyzed Hydration of Epoxides[a]

enzyme/ substrate	k_2 (s^{-1})	k_{-2} (s^{-1})	K_s (mM)	k_2/K_s (M^{-1} s^{-1})	k_3 (s^{-1})	k_4 (s^{-1})	k_{-4} (s^{-1})
MEH[b]							
(2*R*)-**1**	330 ± 50	4.0 ± 1.8	2.0 ± 0.5	(1.7 ± 0.3) × 10^5	0.8 ± 0.1	−	−
(2*S*)-**1**	>300	0.45 ± 0.13	>3	(1.1 ± 0.1) × 10^5	0.07 ± 0.01	−	−
chtMEH							
(2*R*)-**1**	170 ± 13	2.7 ± 0.3	3.2 ± 0.3	(5.2 ± 0.5) × 10^4	0.8 ± 0.1	−	−
(2*S*)-**1**	>200	8.8 ± 2.3	>3	(7.8 ± 0.4) × 10^4	0.11 ± 0.01	−	−
3	24 ± 13	0.5 ± 0.2	0.26 ± 0.1	(9.2 ± 3) × 10^4	0.60 ± 0.24	−	−
chtH431S							
(2*R*)-**1**	27.9 ± 0.5	0.93 ± 0.13	0.29 ± 0.02	(9.3 ± 0.4) × 10^4	−	−	−
(2*S*)-**1**	>80	0.81 ± 0.35	>3	(2.9 ± 0.1) × 10^4	−	−	−
E404Q							
(2*R*)-**1**[c]	230 ± 70	0.15 ± 0.18	1.5 ± 0.5	(1.50 ± 0.01) × 10^5	0.16 ± 0.03	0.014 ± 0.006	0.0062 ± 0.0009
(2*S*)-**1**	>300	∼0	>3	(1.07 ± 0.01) × 10^5	0.0013 ± 0.0004	−	−
chtE404D							
(2*R*)-**1**	>350	7.7 ± 2.4	>3	(1.30 ± 0.01) × 10^5	2.1 ± 0.2	−	−
(2*S*)-**1**	81 ± 6	0.3 ± 0.1	0.9 ± 0.2	(8.8 ± 0.7) × 10^4	0.18 ± 0.01	−	−
chtE376D							
(2*R*)-**1**	310 ± 60	0.9 ± 0.4	5.1 ± 1.2	(6.1 ± 1.2) × 10^4	0.38 ± 0.01	−	−
(2*S*)-**1**	>100	0.1 ± 0.2	>3	(3.7 ± 0.1) × 10^4	0.05 ± 0.01	−	−
chtE376Q[d]							
3	33 ± 15	1.2 ± 0.4	0.26 ± 0.1	(1.3 ± 0.5) × 10^5	0.1 ± 0.02	−	−
chtW150F							
(2*R*)-**1**	400 ± 230	1.4 ± 0.1	3.5 ± 2.7	(1.1 ± 0.4) × 10^5	0.13 ± 0.02	−	−
(2*S*)-**1**	>250	∼0	>3	(8.5 ± 0.2) × 10^4	0.07 ± 0.01	−	−

[a] Values of k_2, k_{-2}, K_s, and k_2/K_s were obtained from the dependence of k_{obs} on the concentration of substrate (for example, see Figure 2). Values of k_3 were obtained from fitting the pre-steady-state and post-steady-state lag phase by numerical integration of the kinetic mechanism (eq 1). [b] Data from (*3*). [c] Values of k_4 and k_{-4} were obtained from a fit of the data to the alternative mechanism (eq 2). [d] Rate constants were estimated by simulation of the time course of the reaction using the KINSIM and FITSIM programs.

1.0 s^{-1} for MEH and chtMEH, respectively. The pre-steady-state kinetic constants for both enantiomers of **1** show detectable though not radical differences as illustrated in Table 1 when the time courses are analyzed assuming the mechanism given in eq 1.

$$E + S \overset{K_s}{\rightleftharpoons} E{\cdot}S \overset{k_2}{\rightleftharpoons} E{-}I \xrightarrow{k_3} E + P \qquad (1)$$

Hydrolysis Reaction: Role of H431 in Catalysis. Several mutations (H431N, H431Q, H431S, H431A, and H431G) at position 431 in the native enzyme were made to probe the role of the residue in catalysis. Virtually all proved very difficult to purify in quantities sufficient for detailed analysis of the pre-steady-state kinetics. One, H431S, was incorporated into the hexahistidine-tag version of the enzyme and proved to be easily purified in reasonable quantities. For this reason, it was chosen for further study. The reason for the sensitivity of the protein to mutations at position 431 is unclear at this juncture.

The chtH431S mutant is not capable of catalyzing the formation of the diol products, **2** and **4**, from **1** and **3**, respectively. Nevertheless, mixing of the chtH431S mutant with either enantiomer of **1** results in a rapid, first-order decrease in the intrinsic fluorescence of the enzyme that is similar to that observed in the native enzyme (*4*, *5*). Unlike the native enzyme, the fluorescence does not recover on extended incubation, indicating that the mutant is alkylated but is incapable of turning over the substrate at an appreciable rate. Although the rate constant (k_2) for the alkylation reaction in the Michaelis complex is somewhat smaller (6-fold) than that of the chtMEH, the efficiency of the reaction (k_2/K_s) is virtually the same (Table 1). The alkylation reaction with (2*R*)-**1** exhibits saturation kinetics (Figure 2) as it does with native MEH and chtMEH. However,

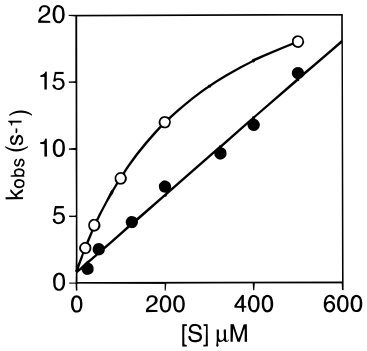

FIGURE 2: Dependence of k_{obs} for the pre-steady-state decrease in fluorescence of the chtH431S mutant on the concentration of (2*R*)-**1** (○) and (2*S*)-**1** (●). The lines for (2*R*)-**1** and (2*S*)-**1** are fits of the experimental data to the equations for a hyperbola {$k_{obs} = k_{-2} + k_2[S]/(K_s + [S])$} and a line ($k_{obs} = k_{-2} + k_2[S]/K_s$), respectively, with the values of the rate constants given in Table 1.

significantly tighter binding of the substrate is observed with the mutant (Table 1). The mutant does not show saturation (Figure 2) with (2*S*)-**1** in the accessible concentration range as was also observed with the native enzyme. The kinetic behavior of chtH431S is exactly that expected from an enzyme lacking the general base necessary to efficiently initiate the hydrolytic half-reaction.

In Search of the Charge Relay Residue. Microsomal epoxide hydrolase exhibits no statistically significant sequence similarity with other α/β-hydrolase fold enzymes in the region suspected of harboring the charge relay residue (residues 340−405). For this reason, we mutated each Asp or Glu residue in this region to the corresponding amide in anticipation that mutation of the charge relay residue would have a minimal effect on the alkylation half-reaction but result in a large reduction in k_{cat} while others would show little or no effect. The results of the mutagenic scan of this

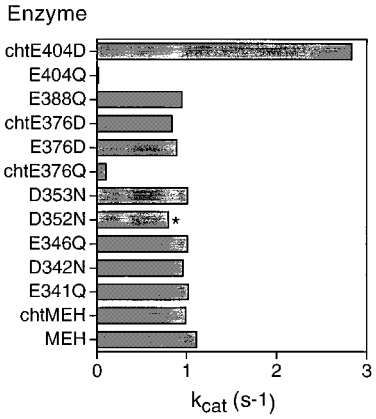

FIGURE 3: Histogram of the turnover numbers of MEH, chtMEH, and carboxylate mutants in the region from residues 340 to 405. All enzymes had a purity of >90% as judged by SDS−PAGE except D352N (*). The observed turnover number for D352N, which was approximately 30% pure, was 0.24 s^{-1}, leading to an estimated turnover number of 0.8 s^{-1}.

region are shown in Figure 3. The enzyme is sensitive to the amide substitution at two of the positions. The chtE376Q and E404Q mutants have turnover numbers of 0.13 s^{-1} and 0.018 s^{-1} toward **3**, respectively, which are significantly smaller than the native enzyme. All other mutants exhibit turnover numbers >0.8 s^{-1}. Interestingly, replacement of E376 or E404 with aspartate either has no effect or, in the case of chtE404D, results in a higher turnover number toward **3**. The sensitivity of k_{cat} to amide substitution suggested that either E376 or E404 or both might serve the charge relay function. For this reason, the pre-steady-state kinetics of both mutants were examined in detail.

Role of E376 in Structure and Catalysis. As indicated under Experimental Procedures, special steps were required to isolate the E376Q mutant. The native enzyme harboring this mutation could not be isolated in significant quantities. The chtE376Q mutant could be isolated in good yield by Ni-chelate chromatography but tended (unlike chtMEH) to precipitate upon removal of the 1 M imidazole required to elute the enzyme from the column. The enzyme appeared to be stabilized by rapid dialysis of the protein against 0.5 M NaCl. For this reason, the pre-steady-state kinetics were performed in buffer containing 0.5 M NaCl. The high salt concentration had no effect on the kinetic behavior of chtMEH.

When the chtE376Q mutant is mixed with either enantiomer of **1**, no change in the protein fluorescence can be observed either at short (<100 ms) or at long reaction times (10 min). Yet the mutant retains detectable catalytic activity with $k_{cat} \geq 0.02$ s^{-1} for (2*R*)-**1** as determined by the HPLC assay (*4*). There are three possible reasons for this curious result. First, the mutant enzyme may be rapidly alkylated but with no concomitant change in the intrinsic protein fluorescence. Second, perhaps only a small fraction of the isolated enzyme is active so that the fluorescence change is too small to observe. Or, third, a change in the rate-limiting step has occurred such that the alkylation reaction is much slower than the hydrolytic half-reaction so that the ester intermediate does not accumulate to an appreciable extent in the steady state.

In an attempt to discriminate among these possibilities, the pre-steady-state kinetics of the reaction of the native and

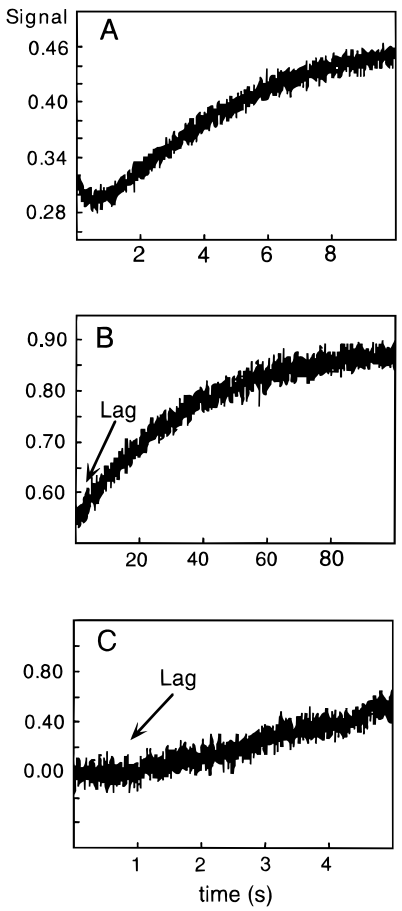

FIGURE 4: Fluorescence change (λ_{ex} = 270 nm, λ_{em} = 320 nm) on rapid mixing of **3** at 25 °C (pH 7) with (A) chtMEH (8 μM enzyme, 8 μM **3**, 6-trace average), (B) chtE376Q (8 μM enzyme, 10 μM **3**, 2-trace average), and chtE376Q (8 μM enzyme, 8 μM substrate, 10-trace average). Note the differences in time scales. The lag in (B) indicated by the arrow is more evident at short reaction times as shown in (C).

mutant enzymes with **3** were investigated. The dihydrodiol of **3** (**4**) is highly fluorescent so that conversion of **3** to the product is accompanied by a large increase in fluorescence at 320 nm (λ_{ex} = 270 nm) (*14*). Mixing of the native enzyme with **3** would be expected to exhibit a rapid change in fluorescence due to alkylation of the enzyme followed by a slower increase due to hydrolysis of the ester to give **4**. The rapid phase could involve either a net increase or a decrease in fluorescence depending on whether the decrease in the intrinsic protein fluorescence or the expected increase due to opening of the oxirane ring dominates the fluorescence of the ester intermediate.

Rapid mixing of chtMEH with **3** in both single- and multiple-turnover experiments results in a rapid, but small, decrease in fluorescence at 320 nm followed by a slower increase to a final value that exceeds the initial intrinsic protein fluorescence. The time course for a single-turnover reaction is illustrated in Figure 4A. The time courses of both single- and multiple-turnover reactions catalyzed by chtMEH can be fit to the simple mechanism of eq 1 with the rate constants shown in Table 1. In contrast, rapid mixing of chtE376Q with **3** results in a slow, increase in fluorescence at 320 nm consistent with a turnover number of about 0.1 s^{-1} (Figure 4B). Although no fast phase is observed, there is a distinct lag before the increase in fluorescence com-

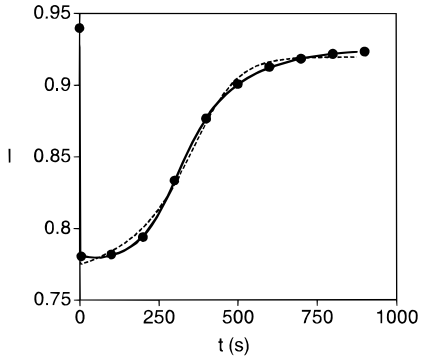

FIGURE 5: Post-steady-state recovery of the intrinsic fluorescence intensity (*I*) for 5.6 μM E404Q reacted with 100 μM (2*R*)-**1**. The solid line is the fit of the experimental points to the mechanism in eq 2 using the program FITSIM and the rate constants in Table 1. The broken line is the best fit of the data to the mechanism of eq 1 using FITSIM.

mences (Figure 4B,C). The time course for hydration of **3** by chtE376Q can be simulated with the rate constants shown in Table 1 assuming that the rapid formation of the ester occurs with no observable change in fluorescence. The only marked difference between the native enzyme and the chtE376Q mutant is seen in k_3, as would be expected if E376 was involved in the hydrolytic half-reaction.

Steady-state kinetic measurements with **3** at pH 8 are also consistent with the above pre-steady-state analysis. The chtE376Q mutant (k_{cat} = 0.13 s^{-1}, K_m = 7.2 μM) behaves very much like the native enzyme (k_{cat} = 1.1 s^{-1}, K_m = 5.5 μM) (*15*) except for the slower turnover. As with the native enzyme, the low value of K_m is a consequence of the fact that in the steady state the ester intermediate is the predominant species. If the E376Q mutation altered the mechanism such that the rate-limiting step was formation of the alkyl-enzyme intermediate, then the apparent K_m value for the substrate would be expected to be much higher, approaching the value of K_s = 260 μM.

Hydrolysis Reaction: Role of E404 in Catalysis. The pre-steady-state kinetic data for the E404Q mutant are clearly consistent with the hypothesis that it is a charge relay residue in the hydrolytic half-reaction (*9*). The mutation has little effect on the alkylation half-reaction with either enantiomer of **1** as indicated in Table 1. On the other hand, there is a significant impairment of the hydrolytic half-reaction with decreases in k_3 by factors of between 5 and 80, depending on the substrate.

Unlike the other enzymes examined in this study, the kinetics of the post-steady-state recovery of fluorescence with the E404Q mutant are not accurately described by the kinetic mechanism in eq 1 as is illustrated in Figure 5. Kinetic simulations of a wide variety of more complex mechanisms lead to the conclusion that the aberration in the recovery of fluorescence is best explained by a reversible dead-end side reaction of the alkyl-enzyme intermediate as illustrated in eq 2.

$$E + S \underset{}{\overset{K_s}{\rightleftharpoons}} E{\bullet}S \underset{k_{-2}}{\overset{k_2}{\rightleftharpoons}} E{-}I \xrightarrow{k_3} E + P \qquad (2)$$

$$E{-}I \underset{k_4}{\overset{k_{-4}}{\rightleftharpoons}} E{-}F$$

Analysis of the fluorescence recovery using this mechanism results in a substantially improved fit of the experimental data as shown in Figure 5. Other possible mechanisms which included additional intermediates along the reaction path or classical product inhibition, for example, did not result in improved fits of the expected kinetic behavior to the experimental data. The possible identity of the dead-end complex E−F is discussed below.

Probing the Oxyanion Hole with W150F. Sequence alignments with other α/β-hydrolase fold enzymes suggest that the main chain NH of W150 is part of the oxyanion hole involved in hydrolysis of the ester (*2, 3, 6, 9*) as illustrated in Figure 1. The location of the tryptophan suggests that it might well contribute to the change in intrinsic fluorescence of the protein upon alkylation. In addition, alterations in the side chain might be expected to affect the efficiency of hydrolysis of the intermediate. The steady-state and pre-steady-state kinetic behavior of the chtW150F mutant is consistent with both of these expectations. The magnitude of the pre-steady-state decrease in fluorescence is about 40% of that exhibited by the native enzyme when alkylated with either enantiomer of **1**. Moreover, the kinetics show that hydrolytic half-reaction occurs 6-fold more slowly with (2*R*)-**1**, though with (2*S*)-**1** it remains unchanged (Table 1). The turnover number of chtW150F toward **3** is 0.1 s^{-1} as compared to the native enzyme of 1 s^{-1}. The modest influence of the side chain on turnover is probably a manifestation of the fact that the effect is not necessarily dependent on the identity of the side chain but on the appropriate positioning of the main chain NH. All of these results are completely consistent with W150 participating as part of the oxyanion hole.

DISCUSSION

Overview of the Mechanistic Features of the Hydrolytic Half-Reaction. The hydrolytic half-reactions of MEH and most other α/β-hydrolase fold enzymes share three mechanistic features that facilitate the hydrolysis of the covalent intermediate, a general base and a charge relay residue which assist in the deprotonation of the attacking water molecule and an oxyanion hole to stabilize the tetrahedral intermediate. Only one of these features, the oxyanion hole, appears in statistically significant local sequence alignments with closely related α/β-hydrolase fold enzymes. The general base, H431, is only apparent in the sequence alignments when additional information such as the mutagenesis studies by Bell and Kasper (*8*) or the knowledge of its expected location in the sequence (about 30 residues from the C-terminus) is taken into account (*1*). Similar topological arguments have been used to suggest that E404 is the charge relay residue in the microsomal enzyme (*9*) even though the sequences show no statistically significant similarities in this region in paired comparisons with other α/β-hydrolase-fold enzymes. The results of the pre-steady-state kinetic analysis of mutants targeted at each of the three structural elements involved in the hydrolytic half-reaction are placed into the context of what is already known about the structure and mechanism of C−X bond hydrolases in the following sections. A unique aspect of this analysis is that, unlike previous studies of soluble epoxide hydrolase (*10, 11*), we demonstrate that mutational replacement of residues involved in the hydrolytic half-reaction impairs, to varying degrees, the decomposition of the intermediate while having only marginal effects on the kinetic competence of the alkylation step.

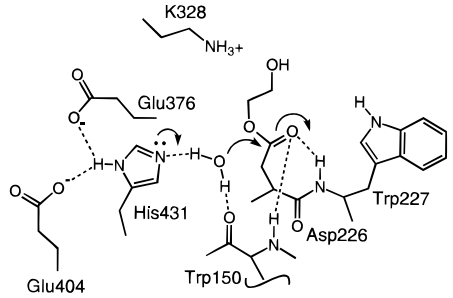

FIGURE 6: Revised proposal for the active site of MEH based on the mutagenesis results reported here and in (*5*). The enzyme is shown poised for the hydrolytic half-reaction. The proposed role of K328 in the alkylation half-reaction remains to be confirmed (*5*).

The Oxyanion Hole. One of the most statistically pronounced features of the sequence alignments among α/*β*-hydrolase fold enzymes that use a carboxylate as the nucleophile is the oxyanion hole. The sequence alignments and the three-dimensional structure of haloalkane dehalogenase are quite informative. The core motif in this region is an HGXP sequence which forms a *cis*-proline reverse-turn projecting the main chain NH of the X residue into the active site where it can hydrogen bond to the carbonyl oxygen and stabilize the tetrahedral intermediate in the hydrolysis of the ester (Figure 6). In the case of MEH, the residue at the X-position is a tryptophan (W150). The properties of the W150F mutant including the reduced change in fluorescence that occurs on alkylation and the somewhat slower hydrolysis of the ester intermediate are clearly consistent with the postulate that W150 is part of the oxyanion hole of MEH. Moreover, the original mutagenic survey of the histidine residues of MEH by Bell and Kasper (*8*) demonstrating that the catalytic efficiency of the enzyme is sensitive to changes in H148 provides additional evidence that the HGXP sequence is part of the oxyanion hole.

The General Base. Although there is little doubt that H431 of MEH acts as the general base in the hydrolysis of the alkyl-enzyme intermediate, the pre-steady state kinetic properties of the chtH431S mutant provide the first quantitative experimental indication that the alkylation and hydrolysis reactions of the epoxide hydrolases can be cleanly dissected by mutagenesis. That is to say, mutations of residues directly involved in one half-reaction have a minimal effect on the other half-reaction. Similar behavior has been recently noted in a bacterial epoxide hydrolase. Rink et al. (*16*) found that mutation of the putative general base (H275) in the epoxide hydrolase from *Agrobacterium radiobacter* AD1 results in an enzyme that appears to form the covalent intermediate but is unable to complete the hydrolysis at an appreciable rate.

The Charge Relay. It is clear that our original guess (*2*) that the charge relay residue of MEH was D352 is incorrect since the D352N mutant is fully active. The experimental results suggest that the charge relay function in microsomal epoxide hydrolase is unique in several respects when compared to the other well-characterized C−X bond hydrolases including soluble epoxide hydrolase, bacterial epoxide hydrolase, and haloalkane dehalogenase. The first difference is that the charge relay function appears to be carried out by a glutamate residue(s) in contrast to the aspartate residues implicated in vertebrate and bacterial epoxide hydrolases (*11, 16*) and haloalkane dehalogenase (*7*). In this regard, MEH is related to other α/*β*-hydrolases which do use a glutamate as the charge relay residue, namely, acetylcholinesterase and triacylglycerol lipase (*1*). The second difference is that as many as two carboxylate groups may be involved in the charge relay function in MEH. Mutational scanning of the region of the cap-domain of MEH suspected of harboring the charge relay residue reveals two residues, E376 and E404, that have the kinetic hallmarks of this function.

The details of the kinetic behavior of the charge relay mutants are what might be expected if two residues shared this function. Note first that mutation of either E376 or E404 to the corresponding carboxamide results in relatively modest decreases (a factor of less than 100) in the rates of hydrolysis of the ester intermediate. In contrast, mutation of the charge relay carboxylate in other epoxide hydrolases typically results in a much more pronounced (>200-fold) decrease in activity (*11, 16*). In fact, Rink et al. (*16*) have suggested that the loss in activity on mutation of the charge relay carboxylate in the *Agrobacterium radiobacter* AD1 epoxide hydrolase is moderated by the presence of another carboxylate (D131) near the active-site histidine. This proposal is mechanistically, though not structurally, analogous to the behavior of the charge relay in MEH proposed here.

Another analogue of the dual charge relay carboxylate can be found in the three-dimensional structure of the triacylglycerol lipase from *Pseudomonas glumae* (*17*). In this instance, one of the two carboxylates, D263, is found to be within hydrogen bonding distance of the general base H285 while the other, E288, is hydrogen bonded to the first carboxylate. Note that the two carboxylate residues flank the general base in the lipase, whereas they both precede the histidine in the sequence of MEH. Whether both glutamate residues of MEH form inner sphere interactions with H431, as is suggested in Figure 6, or if one is involved in an outer sphere interaction as in the example of triacylglycerol lipase is not known. In fact, it is important to point out that although the kinetic results are consistent with both residues performing a charge relay function, they more generally suggest that the two residues are involved in ionic interactions that are important in catalysis. These interactions need not necessarily involve H431.

It seems evident from the results with MEH that a very specific hydrogen bonding geometry between H431 and either E376 or E404 is not required to support catalysis since the E376D and E404D mutants are at least as good if not better than the native enzyme in hydrolysis of the ester (Figure 3, Table 1). Maintaining the charge on either side chain is sufficient to support catalysis. In fact, the E404D mutant is 2−3-fold more efficient at hydrolysis of the ester with the three substrates tested. This is a curious result, suggesting that the native enzyme may not be completely optimized for performing the hydrolytic half-reaction. Could it be that the native enzyme (E404) is in an evolutionary cul-de-sac? Or, is E404 the optimal evolutionary solution for some other reason yet to be determined? In either case, the experimental results suggest that MEH has a unique charge relay system.

The E404Q mutant exhibits a more complex kinetic behavior with (2*R*)-**1** as the substrate. The hydrolysis of the ester seems to involve the reversible formation of a dead-end isomer of the alkyl-enzyme as indicated in eq 2.

Scheme 1

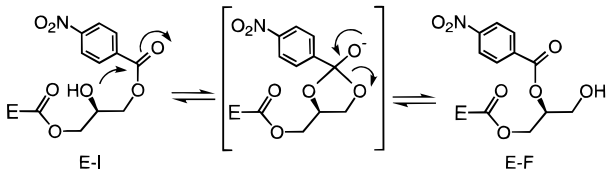

Although the isomerization is detected kinetically, the identity of the isomer remains a matter of speculation. The most likely circumstance is that the ester intermediate undergoes an acyl migration of the type previously described for the diol product, **2** (*5*), as illustrated in Scheme 1. In this regard, it is interesting to note that the magnitudes of the rate constants (k_4 and k_{-4}, eq 2) for the apparent isomerization are not much different than those observed for the acyl migration in **2**, ca. 10^{-3} s^{-1}. Although such acyl migrations might be accelerated, slowed, or prevented by steric constraints in the active site, they would be more likely to occur in mutant enzymes where the hydrolysis of the ester is impaired to the extent that the isomerization becomes a kinetically competitive process.

CONCLUSIONS

The hydrolytic half-reaction of microsomal epoxide hydrolase involves the usual elements of a general base, charge relay, and oxyanion hole expected of enzymes in the α/β-hydrolase fold family. The general base (H431) and one of the key residues in the oxyanion hole (W150), which are apparent in sequence alignments, are essential for efficient hydrolysis of the alkyl-enzyme intermediate but have little influence on the alkylation of the enzyme. The charge relay function appears to be unique in that it is shared by two glutamate residues (E376 and E404) located in or near the cap-domain of the protein. The shared function is manifest in the fact that mutation of either of the residues results in relatively modest decreases in the ability of the enzyme to hydrolyze the alkyl-enzyme intermediate.

REFERENCES

1. Ollis, D. L., Cheah, E., Cygler, M., Dijkstra, B., Frolow, F., Franken, S. M., Harel, M., Remington, S. J., Silman, I., Schrag, J., Sussman, J. L., Verschueren, K. H. G., and Goldman, A. (1992) *Protein Eng. 5*, 197−211.
2. Lacourciere, G. M., and Armstrong, R. N. (1994) *Chem. Res. Toxicol. 7*, 121−124.
3. Lacourciere, G. M., and Armstrong, R. N. (1993) *J. Am. Chem. Soc. 115*, 10466−10467.
4. Tzeng, H.-F., Laughlin, L. T., Lin, S., and Armstrong, R. N. (1996) *J. Am. Chem. Soc. 118*, 9436−9437.
5. Laughlin, L. T., Tzeng, H.-F., Lin, S., and Armstrong, R. N. (1998) *Biochemistry 37*, 2897−2904.
6. Arand, M., Grant, D. F., Beetham, J. K., Friedberg, T., Oesch, F., and Hammock, B. D. (1994) *FEBS Lett. 338*, 251−256.
7. Verschueren, K. H. G., Seljee, F., Rozeboom, H. J., Kalk, K. H., and Dijkstra, B. W. (1993) *Nature 363*, 693−698.
8. Bell, P. A., and Kasper, C. B. (1993) *J. Biol. Chem. 268*, 14011−14017.
9. Beetham, J. K., Grant, D., Arand, M., Garbarino, J., Kiyosue, T., Pinot, F., Oesch, F., Belknap, W. R., Shinozaki, K., and Hammock, B. D. (1995) *DNA Cell Biol. 14*, 61−71.
10. Pinot, F., Grant, D. F., Beetham, J. K., Parker, A. G., Borhan, B., Landt, S., Jones, A. D., and Hammock, B. D. (1995) *J. Biol. Chem. 270*, 7968−7974.
11. Arand, M., Wagner, H., and Oesch, F. (1996) *J. Biol. Chem. 271*, 4223−4229.
12. Barshop, B. A., Wrenn, R. F., and Frieden, C. (1983) *Anal. Biochem. 130*, 134−145.
13. Zimmerle, C. T., and Frieden, C. (1989) *Biochem J. 258*, 381−387.
14. Dansette, P. M., DuBois, G. C., and Jerina, D. M. (1979) *Anal. Biochem. 97*, 340−345.
15. Lacourciere, G. M., Vakharia, V. N., Tan, C. P., Morris, D. I., Edwards, G. H., Moos, M., and Armstrong, R. N. (1993) *Biochemistry 32*, 2610−2616.
16. Rink, R., Fennema, M., Smids, M., Dehmel, U., and Janssen, D. B. (1997) *J. Biol. Chem. 272*, 14650−14657.
17. Noble, M. E. M., Cleasby, A., Johnson, L. N., Egmond, M. R., and Frenken, L. G. J. (1993) *FEBS Lett. 331*, 123−128.

BI9727388